

Compensation of Temperature Effects on Guided Wave Based Structural Health Monitoring Systems

Codrut Alexandru Dan, Pawel Kudela, Wieslaw Ostachowicz

► **To cite this version:**

Codrut Alexandru Dan, Pawel Kudela, Wieslaw Ostachowicz. Compensation of Temperature Effects on Guided Wave Based Structural Health Monitoring Systems. Le Cam, Vincent and Mevel, Laurent and Schoefs, Franck. EWSHM - 7th European Workshop on Structural Health Monitoring, Jul 2014, Nantes, France. 2014. <hal-01020367>

HAL Id: hal-01020367

<https://hal.inria.fr/hal-01020367>

Submitted on 8 Jul 2014

HAL is a multi-disciplinary open access archive for the deposit and dissemination of scientific research documents, whether they are published or not. The documents may come from teaching and research institutions in France or abroad, or from public or private research centers.

L'archive ouverte pluridisciplinaire **HAL**, est destinée au dépôt et à la diffusion de documents scientifiques de niveau recherche, publiés ou non, émanant des établissements d'enseignement et de recherche français ou étrangers, des laboratoires publics ou privés.

COMPENSATION OF TEMPERATURE EFFECTS ON GUIDED WAVE BASED STRUCTURAL HEALTH MONITORING SYSTEMS

C.A. Dan^{a,1}, P. Kudela¹, W. Ostachowicz^{1,2}

¹Polish Academy of Sciences, Institute of Fluid-Flow Machinery, Gdansk, Poland

²Warsaw University of Technology, Faculty of Automotive and Construction Machinery Engineering

^adancodrut@imp.gda.pl

ABSTRACT

The work presented in this paper focuses on the development of analytical methods to compensate for the temperature effects on guided wave propagation. The physical effects of temperature upon the registered signals using piezoelectric sensors mounted in pitch-catch configuration are explored experimentally over considerably large temperature range and frequency bandwidths. The observations made are mathematically interpreted and a mathematical framework which enables a new strategy for compensation of the temperature effects on Lamb waves is formulated. The strategy is validated in an experimental campaign where the plate with the installed SMART Layer is monitored for low temperature differences at room conditions over longer periods of time. Damage scenarios under the form of added mass were considered and the influence of temperature on the damage detection and the efficiency of the proposed strategy are investigated.

KEYWORDS : *Structural Health Monitoring (SHM), Guided Waves, Piezoelectric Sensors, Temperature Effects, Signal Processing.*

Introduction: STRUCTURAL HEALTH MONITORING IN ENVIRONMENTAL CHANGING CONDITIONS

Structural health assessment of structures based on ultrasonic piezoelectric sensors that have the capability to emit and record Lamb waves has developed greatly in recent years. The point has been reached where aerospace manufacturers can acquire complete off the shelf monitoring solutions composed of embeddable sensor networks, acquisition units and necessary software. Pre-established sensor networks can be fitted into composite structures opening the doorway towards permanent health monitoring and remaining service life assessment. In order to reach the desired higher levels of SHM (detection of damage type, extent and life prognosis), strategies relying on a referential subtraction need to be utilized, [1]. Although these strategies pay off in terms of higher level of insight into structural condition, they are highly sensitive to contamination from environmental factors like temperature or moisture. For structures operating under adverse environmental conditions, the process of subtraction between signals accounting for different states of the component induces an inherent noise. These factors affect the structure elastic properties, its density and they greatly affect excitation and sensing ability of transducers. Temperature effects are generally producing large distortions of acoustic propagation through waveguides. Thus, in recent years a great effort has been made by researchers into the attempt to compensate temperature effects, [2]–[6].

Temperature Effects on Guided Waves

Generally acknowledged as a measure of the average molecular internal kinetic energy [7], temperature has a ubiquitous influence upon the macroscopic physical properties of materials, be it electrical, optical, magnetic or, as it will be discussed here, mechanical.

Particularly, solids experience upon change of temperature, modifications in their mechanical properties, of interest being here the elastic and shear moduli and the density, which, in

turn cause changes in the two main elasto-acoustic properties of any given material, acoustical absorption and wave velocity.

Thus, the problem of compensation of temperature effects on guided waves can be split into two smaller problems:

- I. Change in the phase of the recorded time signal with temperature, occurring with the modification of the characteristic wave propagation coefficient (wave speed).
- II. Change in amplitude of the propagating waves with temperature, occurring as a result of the modifications of the characteristic acoustical absorption coefficient (wave attenuation).

While wave speed is independent of attenuation, the reciprocal is not valid, thus a proper strategy would be to compensate for the wave speed and subsequently for the speed-dependent attenuation. The present paper is set to investigate, under the assumption of isotropic and homogeneous materials, the phase change.

Recently, two strategies have been developed also in close contact with real-life situations, Optimal Baseline Selection (OBS) and Baseline Signal Stretch (BSS), [2], [4], [6]. As the names suggest, the two methods are numerical optimisation procedures that rely on the minimisation of the error (environmental noise) in the residual between “damage free” signal and current signal “with damage”. OBS aims to select the best “fit” from a baseline dataset, consisting of signals recorded at the healthy state of a structure at discrete temperatures over a range of interest. BSS aims to find the best “correction” of a baseline recorded at a given temperature for another temperature. The BSS was intended initially as an analytical strategy since it was established on the fundamental physical understanding of the effects of temperature on guided waves [2], but has evolved eventually into a numerical approach [3].

There are several aspects that made the applicability of the analytical stretch onto real complex structures a challenging endeavour:

a. *The time traces stretch with propagation distance.* Any correction of the baseline time-traces using a distance dependent model is difficult with signals containing multiple reflections (usually the case for complex structures). Moreover, even if boundary reflection paths can be determined, reflections of structural features like bolts, rivets or reinforcing elements are difficult and costly to anticipate.

b. *The change in the wave velocities (phase and group) with temperature depends on frequency of the wave.* This statement is, to some extent, the corollary of the previous in that lowering of the wave speed will be perceived by a fixed temporal observer (PZT sensor) as a stretch towards the right of the time axis. The novel part is the remark that the rate of change of wave speed is frequency dependent. In other words, lower frequencies will be less affected by temperature than higher frequencies. This aspect is especially of importance in the context of usage of wave-packets as diagnostic signals. Although this type of interrogation offers improved monitoring capabilities, it also implies that multiple frequencies are present at the same time on the structure (signals exhibit a broad-band spectrum).

Variations to this observation can be found in other studies as well, [2], [3], [8], but have not been considered up to now in baseline-stretch models. It will be shown in the present paper that, under specific and well defined assumptions, this second order change of the wave speed can be predicted with good confidence, and practically implemented.

Experiments

1 EQUIPMENT

An experimental stand consisting of a 1mm aluminium plate instrumented with a rectangular SMART Layer was erected to observe the temperature effects on the damage detection capabilities of the monitoring system, and to validate the proposed models, Fig. 1.

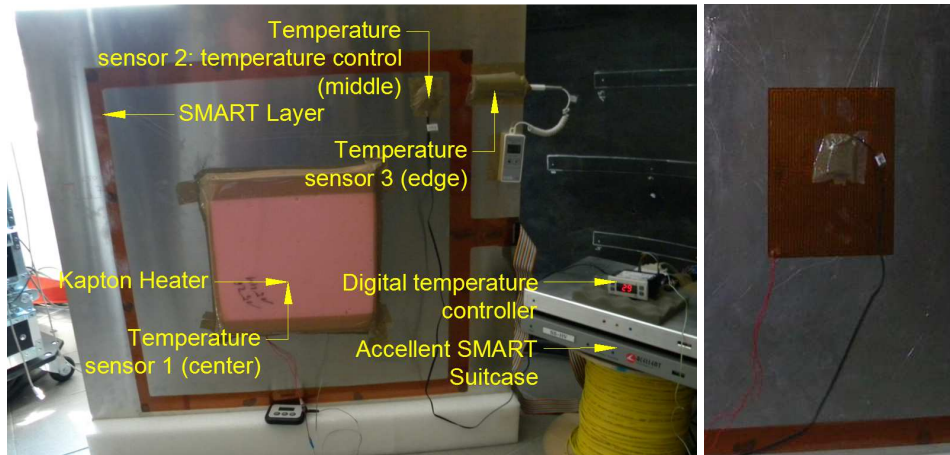


Fig. 1 Temperature measurements set-up (left), KAPTON heater detail (right)

The particular features of this setup include large propagation distances (up to 0.79 m) and the possibility of controlled heating over a large range of temperatures, up to 40°C, but for smaller travelling distances. These characteristics enabled a better insight into the physical phenomena analysed. Both artificial and natural heating (room temperature) were considered. Artificial heating was introduced through a flexible Minco Kapton heater that was placed in the middle of the plate, powered through an 180W DC source and was controlled with a digital thermostat having 1 degree control resolution and 2 degree hysteresis. Temperature was monitored in 3 discrete points, in the centre of the plate on the heater, the edge of plate and one at the middle distance of the two. Lamb waves were recorded over multiple paths of the 12 sensor SMART Layer and for multiple frequencies using the Accellent SMART Suitcase.

2 METHOD

Measurements were taken when the 3 distinct observers showed the same temperature. The temperature was assumed constant over the measured path and during the wave propagation.

Signals were collected for a set of equally spaced frequencies, covering a bandwidth of 50-250 kHz, over two sets of temperature ranges. The large temperature range was generated artificially using the Kapton heater while the small temperature range was obtained naturally.

The large temperature range covered a span of 40°C and included measurement over 1 small sensor distance (0.35m) at intervals of temperature of 1°C.

The small temperature range measurements covered a span of 5°C and included two different distances (0.35m and 0.79m) over the 200kHz bandwidth.

Signals with damage, as well as damage-free were recorded over a small temperature range but for only one frequency (150 kHz) for all the 132 paths available on the SMART Layer.

3 EXPERIMENTAL OBSERVATIONS

Measurements over large temperature range show that the time of arrival change with temperature is linear for the same moment in time, Fig. 2 (middle). On the other hand, the beginning parts of the signal are less affected than the ones accounting for longer time of flight, so the overall effect is perceived as a time-stretch, Fig. 2 (right). This observation is explained theoretically by the Croxford et. al. model. The theoretical model is relating time of arrival with temperature change through the derivation of the speed equation with respect to temperature, see [2].

As stated previously, this approach enables the correction only of first incoming packages, and for a robust detection strategy this is not enough.

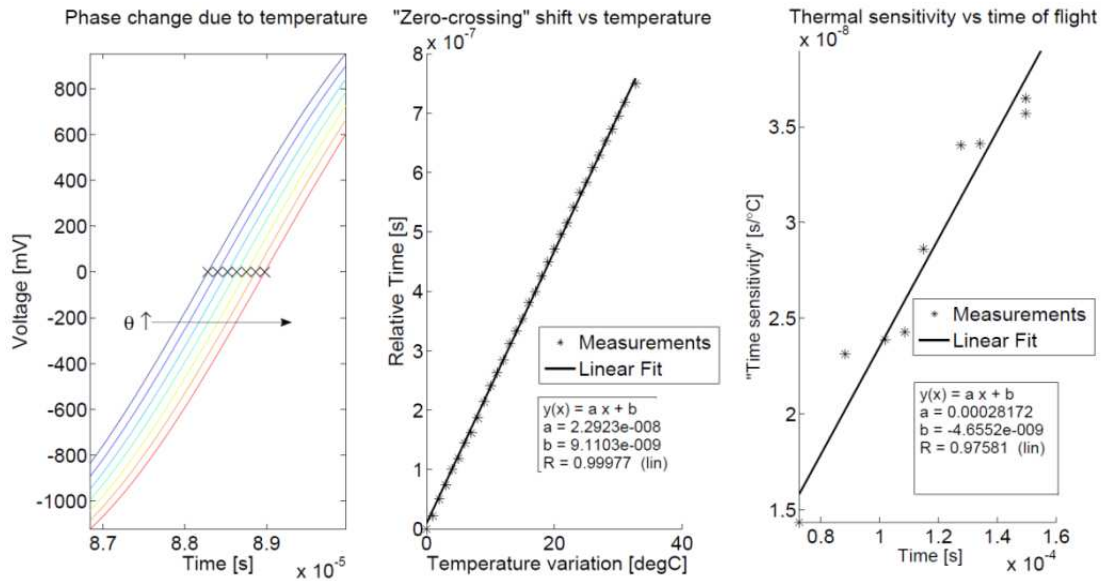


Fig. 2 Detail on phase change recorded at a moment in time (left), linear behaviour of thermally induced time-shift (middle), linear behaviour of time-shift “sensitivity” with time of flight (right)

One way to circumvent the problem of distance dependence in the model is to perform the correction not in the time domain but in the frequency domain. Under the assumption that no additional acoustic sources other than the diagnostic signal are present, it is expected that the actual frequency content of the signal is unaffected by the propagation through the structure. Such an approach to BSS has been previously considered by researchers with good results, [3], [9]. Clarke et al., [3], propose an optimisation strategy that looks for a constant frequency-stretch parameter, Δf , to shift conveniently the spectrum of the baseline in order to minimise the temperature-effects.

Spectra of the signals recorded over the two different distances were analysed and showed that the frequency content of the temperature-affected signals has the same behaviour as the one in time, but of opposite direction. Signals were zero-padded to increase spectral resolution and peaks of signals registered at different temperatures were represented in $f-\Delta\theta$ plots (Fig. 3) that unveil the reversed linearity, allegedly transferred from the time domain.

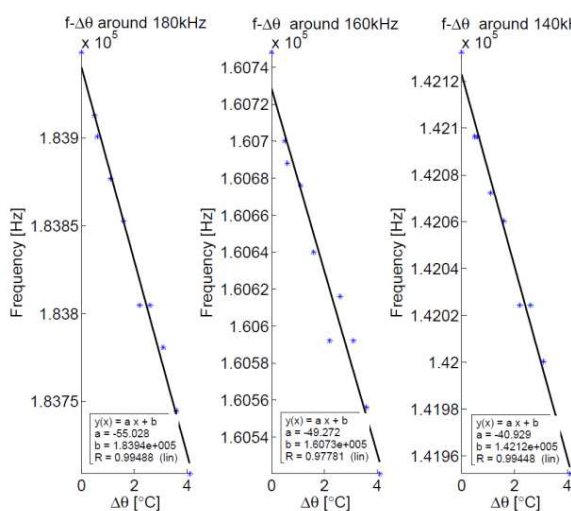


Fig. 3 Frequency drift with temperature for 3 distinct frequencies

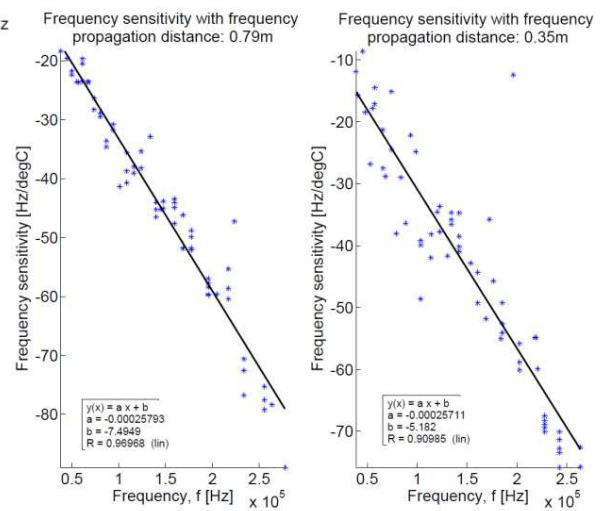


Fig. 4 Frequency thermal sensitivity with frequency over 200kHz band

As previously mentioned, the rate of change of frequency with temperature has been seen to change with frequency. Plots of the recorded frequency sensitivities with respect to temperature unveil the linear characteristic of this change, Fig. 4. An important observation at this point is that the second order dependency, the slope of the frequency sensitivity versus frequency line, is not dependent upon the propagation distance.

Mathematical Framework

1 THE FREQUENCY-TEMPERATURE MODEL

The experiments revealed that,

$$\frac{d\omega}{d\theta} = \xi, \text{ (Fig. 3)} \quad \text{(Eq. 1)}$$

and that

$$\frac{d\xi}{d\omega} = \zeta, \text{ (Fig. 4)} \quad \text{(Eq. 2)}$$

Where

ξ – the frequency sensitivity to temperature, $\left[\frac{\text{Hz}}{^\circ\text{C}}\right]$;

ζ – the coefficient of change of frequency sensitivity to temperature with frequency, $\left[\frac{\text{Hz}}{\text{Hz}\cdot^\circ\text{C}}\right]$

Note that the expressions are in terms of angular frequency, $\omega = 2\pi f$, in order to further correlate with established theory. Also, the insensitivity of the ζ parameter to propagation distance enables the frequency-based analysis.

Integration of (Eq. 2) and subsequent substitution in (Eq. 1), yields that

$$\frac{d\omega}{d\theta} = \zeta\omega + A, \quad \text{(Eq. 3)}$$

This shows that the rate of change of frequency with temperature is proportional with frequency. Separating the variables and integrate of (Eq. 3) over the limits: θ from θ_0 to θ and ω from ω_0 to $\omega(\theta)$, leads to the frequency-temperature solution function

$$\omega(\theta) = \frac{1}{\zeta} [(\zeta \cdot \omega_0 + A) \cdot e^{\zeta \cdot \Delta\theta} - A], \quad \text{(Eq. 4)}$$

Where,

$\omega(\theta)$ - frequency dependency on temperature;

ω_0 - frequency at initial temperature θ_0 , [Hz];

$\Delta\theta$ – difference in temperature, $\theta - \theta_0$, [$^\circ\text{C}$];

ζ – the coefficient of change of frequency sensitivity to temperature with frequency, $\left[\frac{\text{Hz}}{\text{Hz}\cdot^\circ\text{C}}\right]$.

Experimentally, ζ was found to be $\zeta_{Al} = -2.57 \cdot 10^{-4} \frac{\text{Hz}}{\text{Hz}\cdot^\circ\text{C}}$ (Fig. 4).

A – an arbitrary integration constant.

2 IMPLEMENTATION OF FREQUENCY-TEMPERATURE MODEL

A detailed development of Rayleigh-Lamb Equations can be found in [10].

Our temperature analysis starts with two wave equations of the partial scalar and vector potentials Φ and Ψ of the displacement field. The main observation is that, with temperature, the coefficients of the wave equation become temperature-variant. The variable-coefficient wave equation problem is a common one in both classical and quantum mechanics and has been addressed in many sources, [11], [12], but never to solve the temperature effects on Rayleigh-Lamb elastic waves. The main idea is that, for specific speed profiles of $c_L(\Delta\theta)$ and $c_T(\Delta\theta)$, the variable-coefficient wave equation can be reduced, via a change of variables, to a constant coefficient wave equation, i.e.

$$\nabla^2 \Phi = \frac{1}{c_L(\Delta\theta)^2} \frac{\delta^2 \Phi}{\delta t^2} \text{ becomes } \nabla^2 \Phi^\theta = \frac{1}{c_L(\theta_0)^2} \frac{\delta^2 \Phi^\theta}{\delta t^2} \quad \text{(Eq. 5)}$$

and

$$\nabla^2\Psi = \frac{1}{c_T(\Delta\theta)^2} \frac{\delta^2\Psi}{\delta t^2} \text{ becomes } \nabla^2\Psi^\theta = \frac{1}{c_T(\theta_0)^2} \frac{\delta^2\Psi^\theta}{\delta t^2} \tag{Eq. 6}$$

Where,

$\Delta\theta$ is the temperature change $\Delta\theta = \theta - \theta_0$

c_L and c_T are the wave velocities at a reference temperature, θ_0 and

Φ^θ and Ψ^θ are the new change of variable functions with $\Phi \rightarrow \Phi^\theta(\Phi, \Delta\theta)$ and $\Psi \rightarrow \Psi^\theta(\Psi, \Delta\theta)$.

The development continues further as known, but with the new variables Φ^θ and Ψ^θ . By reducing the system to 2 dimensions and assuming harmonic solutions to the wave equation,

$$\Phi^\theta = \Phi^\theta(x_3)\exp(i(k^\theta x_1 - \omega^\theta t)) \tag{Eq. 7}$$

$$\Psi^\theta = \Psi^\theta(x_3)\exp(i(k^\theta x_1 - \omega^\theta t)) \tag{Eq. 8}$$

Where x_1 and x_3 are the spatial domains and t is the time domain and $k \rightarrow k^\theta = k^\theta(k, \Delta\theta)$ and $\omega \rightarrow \omega^\theta = \omega^\theta(\omega, \Delta\theta)$ are the new wavenumber and angular frequencies as functions of reference temperature wavenumber and angular frequency and temperature change. The insertion of the assumed solutions, (Eq. 7) and (Eq. 8), into the wave equations (Eq. 5) and (Eq. 6) will yield the new Rayleigh-Lamb equations with temperature-dependent variables.

To predict the behaviour of the Lamb waves at a given temperature θ knowing the behaviour at θ_0 , it is necessary to implement the frequency-temperature model into the new-variable Rayleigh-Lamb equations, that is, to solve for k^θ using $\omega^\theta = \omega^\theta(\omega, \Delta\theta)$. Fig. 5 shows a comparison between variable-coefficient frequency spectra and the reduced constant coefficient frequency spectra. For the determination of the variable coefficient curves, known aluminium coefficients of temperature dependency (Young modulus: $\alpha_E = 4.8 \cdot 10^{-4}[1/^\circ\text{C}]$, shear modulus: $\alpha_G = 5.2 \cdot 10^{-4}[1/^\circ\text{C}]$, density: $\alpha_\rho = 7.5 \cdot 10^{-5}[1/^\circ\text{C}]$, [13]) were utilised to find c_L and c_T at different temperatures. Constant variable curves were determined as presented above using the experimentally observed frequency-sensitivity parameter ζ , see (Eq. 4).

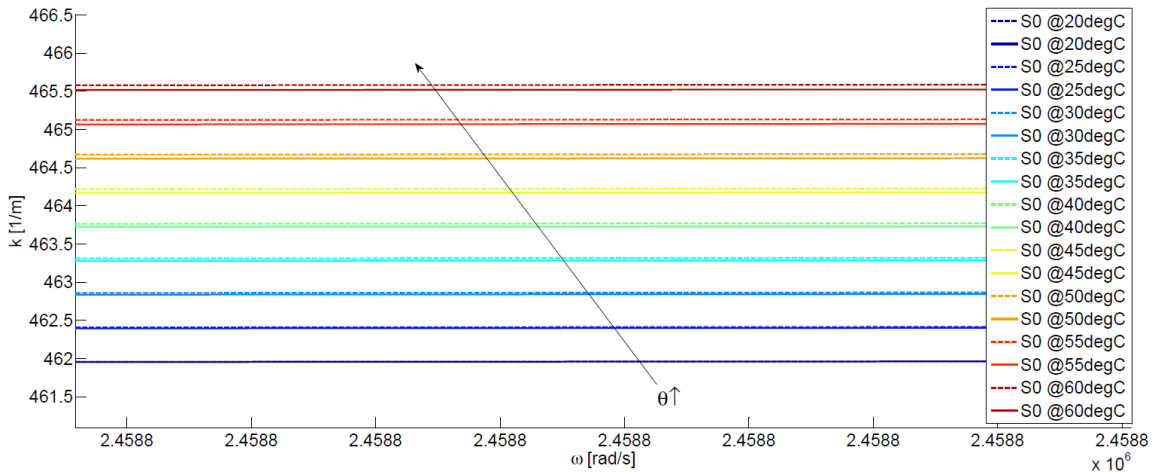


Fig. 5 Constant coefficient Lamb waves frequency spectra (dashed) versus variable-coefficient frequency spectra(filled) for the S0 mode

Lamb-wave signal correction

The aim of the temperature compensation through signal stretch is to correct a temperature-affected differential to retrieve the damage information that can be concealed by the environmental

noise. Fig. 6 shows that the compensation strategy proposed improved by an average of -14 dB the residual resulting from subtraction of two sets of data registered on undamaged plate, but at a 4°C temperature difference.

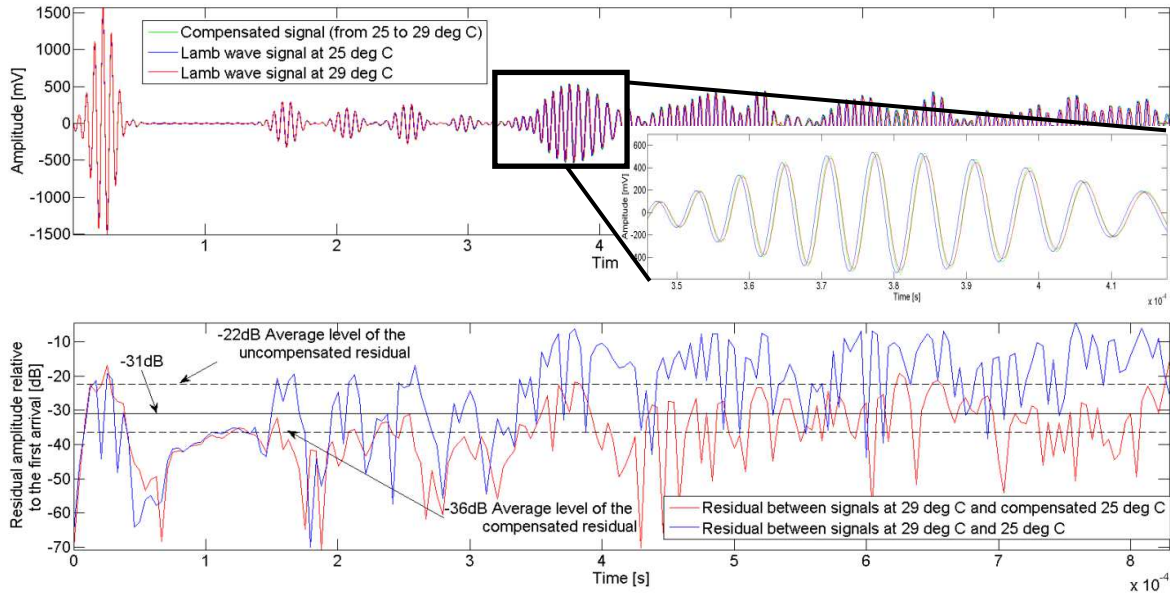


Fig. 6 Temperature compensation of Lamb-wave signals

A damage scenario was simulated under the form of an added mass on the aluminium plate. Signals were collected at different temperatures with and without the added mass. Differentials between the damaged state and baselines at different temperatures are compared with the proposed correction, Fig. 7. The first incursion above the noise floor at ~160 μs travel time represents the arrival of the damage-reflected package. It can be clearly seen that only two degrees of temperature difference between the baseline and the damage state produce enough environmental noise to cover-up the damage reflection. Because such temperature changes are expected to occur naturally, maybe even during different moments of the same day, it can be concluded that temperature compensation of guided wave based supervised SHM systems is compulsory for components exposed to environmental conditions.

Moreover, the figure shows that the proposed strategy manages to bring the differential back to the levels required for damage detection, for the particular case of S0 mode propagation on a 1mm Al plate. Further developments are required for extension for A0-based damage detection.

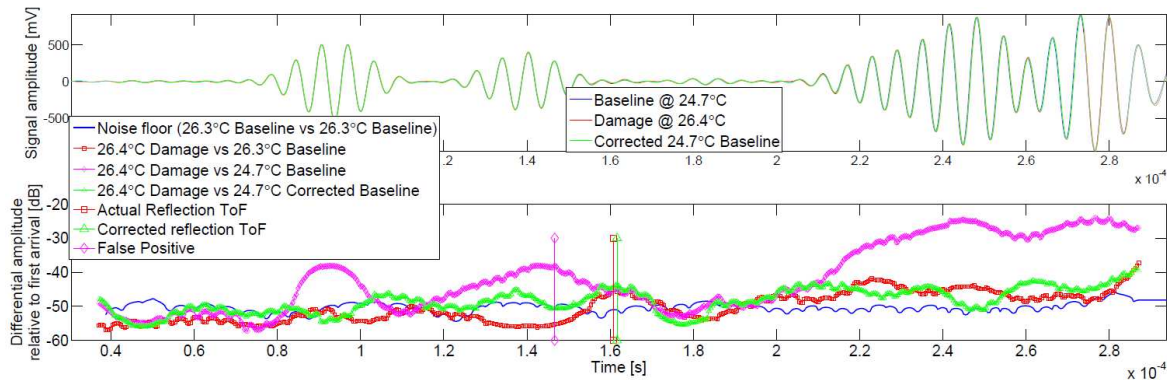


Fig. 7 Temperature effects on SHM

Conclusions

Temperature compensation of guided wave based supervised SHM systems is compulsory for components exposed to environmental conditions.

A new compensation strategy for the temperature effects on Lamb waves was introduced. The signal-stretch method allows the prediction of the Lamb wave behaviour with temperature without prior knowledge on the temperature dependencies of the material properties.

For the given setup, the proposed signal processing improved by an average of -14 dB the residual resulting from subtraction of two sets of data recorded at a 4°C temperature difference.

The strategy is validated on an off-the shelf SHM system. It has been shown that the correction of the thermally-induced phase distortion alone ensures the necessary level of compensation for an S0 based damage detection for the 1mm aluminium plate.

The model needs to be complemented with amplitude correction in order to extend the procedure to the more sensitive A0 mode and to reach the desired levels of SHM robustness.

Acknowledgements

The authors would like to acknowledge the EU Commission support for this research conducted under a Marie Curie Fellowship founded through IMESCON project, grant no. 264672.

References

- [1] K. Worden, C. R. Farrar, G. Manson, and G. Park, "The fundamental axioms of structural health monitoring," *Proc. R. Soc. A Math. Phys. Eng. Sci.*, vol. 463, no. 2082, pp. 1639–1664, Jun. 2007.
- [2] A. J. Croxford, P. D. Wilcox, B. W. Drinkwater, and G. Konstantinidis, "Strategies for guided-wave structural health monitoring," *Proc. R. Soc. A Math. Phys. Eng. Sci.*, vol. 463, no. 2087, pp. 2961–2981, Nov. 2007.
- [3] T. Clarke, F. Simonetti, and P. Cawley, "Guided wave health monitoring of complex structures by sparse array systems: Influence of temperature changes on performance," *J. Sound Vib.*, vol. 329, no. 12, pp. 2306–2322, Jun. 2010.
- [4] Y. Lu and J. E. Michaels, "A methodology for structural health monitoring with diffuse ultrasonic waves in the presence of temperature variations.," *Ultrasonics*, vol. 43, no. 9, pp. 717–31, Oct. 2005.
- [5] A. J. Croxford, J. Moll, P. D. Wilcox, and J. E. Michaels, "Efficient temperature compensation strategies for guided wave structural health monitoring.," *Ultrasonics*, vol. 50, no. 4–5, pp. 517–28, Apr. 2010.
- [6] G. Konstantinidis, P. D. Wilcox, and B. W. Drinkwater, "An Investigation Into the Temperature Stability of a Using Permanently Attached Sensors," vol. 7, no. 5, pp. 905–912, 2007.
- [7] T. H. Barron, *Thermal Expansion of Solids, (Chapter1: Generalized Theory of Thermal Expansion of Solids)*, I. Materials Park, OH: ASM International, 1998, pp. 1–109.
- [8] G. Konstantinidis, B. W. Drinkwater, and P. D. Wilcox, "The temperature stability of guided wave structural health monitoring systems," *Smart Mater. Struct.*, vol. 15, no. 4, pp. 967–976, Aug. 2006.
- [9] T. Clarke, F. Simonetti, S. Rokhlin, P. Cawley, D. O. Thompson, and D. E. Chimenti, "Evaluation of the Temperature Stability of a Low-Frequency A0 Mode Transducer Developed for Shm Applications," *AIP Conf. Proc.*, vol. 975, pp. 910–917, 2008.
- [10] J. L. Rose, *Ultrasonic waves in solid media*. Cambridge, UK: Cambridge University Press, 2004.
- [11] R. Grimshaw, D. Pelinovsky, and E. Pelinovsky, "Homogenization of the variable-speed wave equation," *Wave Motion*, vol. 47, no. 8, pp. 496–507, Dec. 2010.
- [12] B. G., "On mapping linear partial differential equations to constant coefficient equations," *SIAM J. Appl. Math.*, no. 43, pp. 1259–1273, 1983.
- [13] K. & Laby, *Tables of Physical and Chemical Constants*, 15th ed. Essex, UK: Longman Group Limited, 1986, pp. 31–36.